Article

Differential Conductance Switching of Planar Tunnel Junctions Mediated by Oxidation/Reduction of Functionally Protected Ferrocene

Jose A. M. Dinglasan, Michael Bailey, Jong B. Park, and Al-Amin Dhirani

J. Am. Chem. Soc., **2004**, 126 (20), 6491-6497• DOI: 10.1021/ja0394176 • Publication Date (Web): 29 April 2004

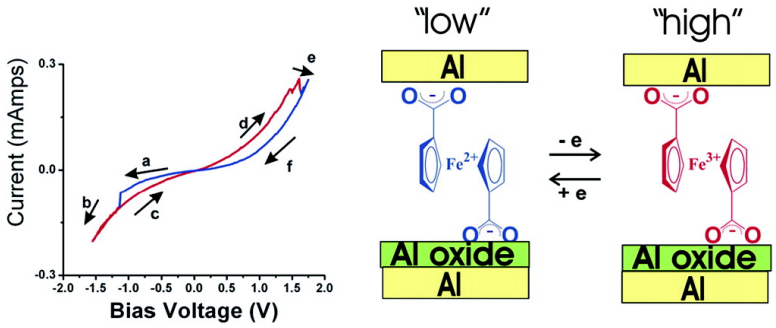

More About This Article

Additional resources and features associated with this article are available within the HTML version:

- Supporting Information
- Links to the 1 articles that cite this article, as of the time of this article download
- Access to high resolution figures
- Links to articles and content related to this article
- Copyright permission to reproduce figures and/or text from this article

View the Full Text HTML

J|A|C|S
ARTICLES
Published on Web 04/29/2004

Differential Conductance Switching of Planar Tunnel Junctions Mediated by Oxidation/Reduction of Functionally Protected Ferrocene

Jose A. M. Dinglasan, Michael Bailey, Jong B. Park, and Al-Amin Dhirani*

Contribution from the Department of Chemistry, University of Toronto, 80 St. George Street, Toronto, Ontario, Canada M5S 3H6

Received November 4, 2003; E-mail: adhirani@chem.utoronto.ca

Abstract: Planar tunnel junctions were fabricated by self-assembling 1,1′- ferrocenedicarboxylic acid (FDCA) onto native oxides of thermally deposited aluminum films and subsequently depositing a second aluminum film. Junctions were characterized using Reflection−Absorption Fourier Transform Infrared Spectroscopy (RAIRS) and current−voltage (*I*−*V*) spectroscopy. Before deposition of the second aluminum film, RAIRS of FDCA and ferrocenecarboxylic acid (FCA) films revealed COO^-, C═O, and Fc ring stretching modes, indicating that both types of molecules can interact strongly with the oxide and remain intact. After deposition, systems exhibited prominent COO^- modes and weakened C═O modes, indicating further reaction with aluminum/aluminum oxide. Fc ring modes persisted in FDCA systems but disappeared in FCA systems, suggesting that the second COOH group in the FDCA molecule can act as a protecting group for the ferrocene moiety. Cyclic *I*−*V* measurements of FDCA tunnel junction systems revealed very strong (∼10-fold) hysteretic differential conductance switching that was both reversible and stable. Control measurements using as prepared junctions, as well as junctions containing 1,6-hexanedioic acid, 1,9-nonanedioic acid, 1,4-dibenzoic acid, or FCA revealed only very weak (∼10%) differential conductance changes. We attribute FDCA junction switching to barrier profile modifications induced by oxidation/reduction of the functionally protected ferrocene moieties.

Introduction

Planar tunnel junctions (PTJs) are a very attractive platform for investigating a wide variety of molecular electronic behaviors and for exploring their potential device applications.[1−37] PTJs are straightforward to fabricate and are cost-effective. They are scalable, potentially down to molecular levels.[25,33] They are also extremely sensitive to barrier structure, and therefore, their

(1) Jaklevic, R. C.; Lambe, J. *Phys. Rev. Lett.* **1966**, *17*, 1139.
(2) Fisher, J. C.; Giaever, I. *J. Appl. Phys.* **1961**, *32*, 172.
(3) Polymeropoulos, E. E.; Sagiv, J. *J. Chem. Phys.* **1978**, *69*, 1836.
(4) Potember, R. S.; Poehler, T. O.; Cowan, D. O. *Appl. Phys. Lett.* **1979**, *34*, 405.
(5) Kevorkian, J.; Labes, M. M.; Larson, D. C.; Wu, D. C. *Discuss. Faraday Soc.* **1971**, *51*, 139.
(6) Kasica, H.; Wlodarski, W.; Kurczewska, H.; Szymanski, A. *Thin Solid Films* **1975**, *30*, 325.
(7) Szymanski, A.; Larson, D. C.; Labes, M. M. *Appl. Phys. Lett.* **1969**, *14*, 88.
(8) Chabinyc, M. L.; Chen, X.; Holmlin, R. E.; Jacobs, H.; Skulason, H.; Frisbie, C. D.; Mujica, V.; Ratner, M.; Rampi, M. A.; Whitesides, G. M. *J. Am. Chem. Soc.* **2002**, *124*, 11730.
(9) Bandhopadhyay, A.; Pal, A. J. *J. Phys. Chem. B* **2003**, *107*, 2531.
(10) Bandhopadhyay, A.; Pal, A. J *Appl. Phys. Lett.* **2003**, *82*, 1215.
(11) Dinglasan, J. A. M.; Shivji, A.; Dhirani, A.-A. *J. Chem. Phys.* **2003**, *119*, 5654.
(12) McCreery, R.; Dieringer, J.; Solak, A. O.; Snyder, B.; Nowak, A. M.; McGovern, W. R.; DuVall, S. *J. Am. Chem. Soc.* **2003**, *125*, 10748.
(13) Solak, A. O.; Eichorst, L. R.; Clark, W. J.; MrCreery, R. L. *Anal. Chem.* **2003**, *75*, 296.
(14) Boulas, C.; Davidovits, J. V.; Rondelez, F.; Vuillame, D. *Phys. Rev. Lett.* **1996**, *76*, 4797.
(15) Vuillaume, D.; Boulas, C.; Collet, J.; Davidovits, J. V.; Rondelez, F. *Appl. Phys. Lett.* **1996**, *69*, 1646.
(16) Vilan, A.; Shanzer, A.; Cahen, D. *Nature* **2000**, *404*, 166.
(17) Wu, D. G.; Ghabboun, J.; Martin, I. M. L.; Cahen, D. *J. Phys. Chem. B* **2001**, *105*, 12011.
(18) Cohen, R.; Kronik, L.; Shanzer, A.; Cahen, D.; Liu, A.; Rosenwaks, Y.; Lorenz, J. K.; Ellis, A. B. *J. Am. Chem. Soc.* **1999**, *121*, 10545.
(19) Vilan, A.; Ghabboun, J.; Cahen, D. *J. Phys. Chem. B* **2003**, *107*, 6360.
(20) Kushida, M.; Inomata, H.; Tanaka, Y.; Harada, K,; Saito, K.; Sugita, K. *Jpn. J. Appl. Phys.* **2002**, *41*, L281.
(21) Kushida, M. Inomata, H.; Miyata, H.; Harada, K.; Saito, K.; Sugita, K. *Jpn. J. Appl. Phys.* **2003**, *42*, L622.
(22) Metzger, R. M. *Chem. Rev.* **2003**, *103*, 3803.
(23) Wong, E. W.; Collier, C. P.; Behloradsky, M.; Raymo, F. M.; Stoddart, J. F.; Heath, J. R. *J. Am. Chem. Soc.* **2000**, *122*, 5831
(24) Donhauser. Z. J.; Mantooth, B. A.; Kelly, K. F.; Bumm, L. A.; Monnel, J. D.; Stapleton, J. J,; Price, D. W, Jr.; Allara, D. L.; Tour, J. M.; Weiss, P. S. *Science* **2001**, *292*, 2303.
(25) Collier, C. P.; Mattersteig, G.; Wong, E. W.; Luo, Y.; Beverly. K.; Sampaio, J.; Raymo, F. M.; Stoddart, J. F.; Heath, J. R. *Science* **2000**, *289*, 1172.
(26) Pease, A. R.; Jeppesen, J. O.; Stoddart, J. F.; Luo, Y.; Collier, C. P.; Heath, J. R. *Acc. Chem. Res.* **2001**, *34*, 433.
(27) Luo, Y. Collier, C. P.; Jeppesen, J. O.; Nielsen, K. A.; Delonno, E.; Ho, G.; Perkins, J.; Tseng, H.-R.; Yamamoto, T.; Stoddart, J. F.; Heath, J. R. *Chem. Phys. Chem.* **2002**, *3*, 519.
(28) Collier, C. P.; Ma, B.; Wong, E. W.; Heath, J. R.; Wudl, F. *Chem. Phys. Chem.* **2002**, *3*, 458.
(29) Chen, Y.; Jung, G.-Y.; Ohlberg, D. A. A.; Li, X.; Stewart, D. R.; Jeppsen, J. O.; Nielsen, K. A.; Stoddart, J. F.; Williams, R. S. *Nanotechnology* **2003**, *14*, 462.
(30) Reed, M. A.; Chen, J.; Rawlett, A. M.; Price, D. W.; Tour, J. M. *Appl. Phys. Lett.* **2001**, *78*, 3735.
(31) Wang, W.; Lee, T.; Reed, M. A. *Phys. E* **2003**, *19*, 117.
(32) (a) Chen, J.; Reed, M. A. *Chem. Phys.* **2002**, *281*, 127. (b) **.** Chen, J.; Calvet, L. C.; Reed, M. A.; Carr, D. W.; Grubisha, D. S.; Bennett, D. W, *Chem. Phys. Lett.* **1999**, *313*, 741.
(33) Chen, J.; Reed, M. A.; Rawlett, A. M.; Tour, J. M. *Science* **1999**, *286*, 1550
(34) Chen, J.; Wang, W.; Klemic, J.; Reed, M. A.; Axelrod, B. W.; Kaschak, D. M.; Rawlett, A. M.; Price, D. W.; Dirk, S. M.; Tour, J. M.; Grubisha, D. S.; Bennett, D. W. *Ann. N.Y. Acad. Sci.* **2002**, *960*, 69.
(35) Wang, W.; Lee, T.; Kamdar, M.; Reed, M. A.; Stewart, M. P.; Hwang, J.-J.; Tour, J. M. *Superlat. Microstruct.* **2003**, *33*, 217.
(36) Kornilovich, P. E.; Bratkovsky, A. M.; Williams, R. S. *Phys. Rev. B* **2002**, *66*, 245413.

behavior can be tuned by doping junctions with suitably designed molecular architectures.

Molecule-induced bistable switching of PTJs is of particular interest in molecular electronics since electrically actuated switches are among the most basic components for memory and logic.[34,36] At high voltages (on the order of at least 3 V), as prepared rf sputtered and thermally annealed aluminum oxide PTJs [38,39] are also known to exhibit switching phenomena; however, these phenomena tend to be associated with uncontrolled junction breakdown, semipermanent phase transitions within the metal−insulator−metal structure, or from filling and emptying of impurity or defect trap states within the oxide film.[40] Molecular film mediated memory and switching effects have been observed in junctions comprising semiconducting, polycrystalline CuTCNQ films sandwiched between Cu and Al electrodes[4] and junctions containing p-quaterphenyl and tetracene thin films sandwiched between gold and/or aluminum electrodes.[5−7] In these junctions, switching and memory phenomena arose from bulk film effects, such as field and/or thermally assisted film restructuring and metal filament formation. The desired switching effect was induced by a relatively high voltage, eventually leading to junction breakdown. Differential conductance switching and bistable memory effects arising from specific molecular architectures have recently been reported using junctions containing Rose Bengal and similarly structured conjugated organic dyes,[9−10,20−21] catenanes,[25−26] rotaxanes,[23,26] self-assembled redox-active phenylene ethynylene oligomers,[30−35] and nitroazobenzene monolayers.[12,13] In all cases, charge injection or removal is thought to occur. In some cases, the charges are thought to become trapped in metastable states through an initial voltage pulse and to become untrapped over time thermally or through subsequent voltage pulses.[30−35] In other cases, oxidation/reduction is thought to give rise to stable and reversible mechanochemical,[25] conformational,[33] or bond conjugation changes in the molecule.[9,10] The changes in turn give rise to hysteretic differential conductance switching. Although the various underlying switching mechanisms are still being investigated, these studies clearly illustrate a potential of conductance switching to molecular electronics.

A challenge that often arises when rationalizing PTJ device behavior is that junctions are typically fabricated by thermally depositing a metal, such as gold, silver, aluminum, titanium, or chromium, on top of the molecules.[33] The deposition of a top metal electrode frequently alters the chemical identity of underlying molecules[12,41,43−45] and can obscure correlations between molecular structure and observed junction properties/characteristics. Titanium and chromium, for example, are reactive to surface alkyl groups and lead to a formation of interfacial TiC_x species[41] while gold can percolate through alkane chains.[42] A promising solution is to exploit terminal molecular functional groups that are reactive with the top metal electrode and that can protect underlying molecular architectures.[12,23,25,43] Suitable functional group−metal combinations include thiol−gold as well as carboxylic acids− or esters−aluminum. [41−45]

Chart 1

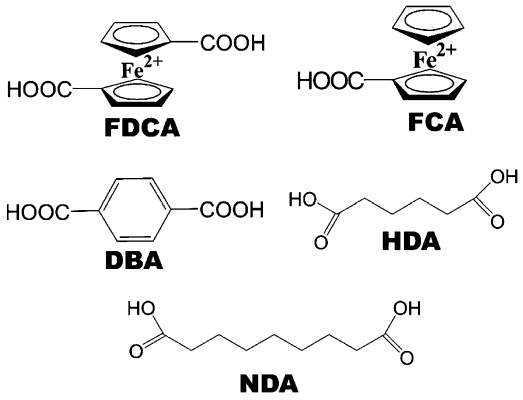

In the present study, we report on differential conductance switching of PTJs with suitably protected ferrocene monolayers. Ferrocene derivatives represent a target of opportunity in a context of conductance switching for a number of reasons.[46] The ferrocene moiety is a simple, prototype system. Redox activities of ferrocene and its various derivatives have been extensively studied, and ferrocene itself is often used as a redox standard.[47,48] Its various derivatives are easily obtained commercially. Also, ferrocene moieties are very robust systems. Their redox states and derivatives can exhibit remarkable chemical as well as thermal stability up to ∼500 °C. In the present study, we present Reflection−Absorption Fourier Transform Infrared Spectroscopy (RAIRS) measurements of 1,1′-ferrocenedicarboxylic acid (FDCA, Chart 1), demonstrating that the two carboxylic acid groups serve (1) to enhance chemical interactions with an aluminum oxide surface through the formation of a carboxylate-aluminum oxide bond and (2) to protect the ferrocene moiety from an aluminum overlayer. Electrical measurements of FDCA junctions show ∼10-fold differential conductance switching which is stable and reversible hysteretic and which, based on control measurements, we attribute to oxidation/reduction of the protected ferrocene moiety. Due to their rich redox activity, we believe that organometallics in general, and ferrocene-based compounds in particular, are a promising new test bed for exploring PTJ conductance switching and nanoscale molecule−metal charge-transfer processes.

Experimental Section

Tunnel junctions were fabricated by resistively evaporating a 3−5 nm chromium adhesion layer (chromium coated tungsten rod, Kurt J. Lesker) and subsequently a 100−150 nm thick aluminum film (99.99%

(37) Adams, D. M.; Brus, L.; Chidsey, C. E.; Creager, S.; Creutz, C.; Kagan, C. R.; Kamat, P. V.; Lieberman, M.; Lindsay, S.; Marcus, R. A.; Metzger, R. M.; Michel-Beyerle, M. E.; Miller, J. R.; Newton, M. D.; Rolison, D. R.; Sankey, O. Schanze, K. S.; Yardley, J.; Zhu, X. *J. Phys. Chem. B* **2003**, *107*, 6668.
(38) Rahman, A.; Raven, M. S. *Thin Solid Films* **1980**, *71*, 7.
(39) Bardhan, A. R.; Srivastava, P. C.; Bhattacharya, D. L. *Thin Solid Films* **1974**, *24*, S41.
(40) Kurnosikov, O.; de Nooij, F. C.; LeClair, P.; Kohlhepp, J. T.; Koopmans, B.; Swagton, H. J. M.; de Jonge, W. J. M. *Phys. Rev. B* **2001**, *64*, 153407-1.
(41) Konstadinidis, K.; Zhang, P.; Opila, R. L.; Allara, D. L. *Surf. Sci.* **1995**, *388*, 300.
(42) (a) Ohgi, T.; Sheng, H.-Y.; Nejoh, H. *Appl. Surf. Sci.* **1998**, *130−132*, 919. (b) Ohgi, T.; Sheng, H.-Y.; Dong, Z.-C.; Nejoh, H. *Surf. Sci.* **1999**, *442*, 277.
(43) Hooper, A.; Fisher, G. L.; Konstadinidis, K.; Jung, D.; Nguyen, H.; Opila, R.; Collins, R. W.; Winograd, N.; Allara, D. L. *J. Am. Chem. Soc.* **1999**, *121*, 8052.
(44) Haynie, B. C.; Walker, A. V.; Tighe, T. B.; Allara, D. L.; Winograd, M. *Appl. Surf. Sci.* **2003**, *203−204*, 433.
(45) (a) Fisher, G. L.; Walker, A. V.; Hooper, A. E.; Tighe, T. B.; Bahnck, K. B.; Skriba, H. T.; Reinard, M. D.; Haynie, B. C.; Opila, R. L.; Winograd, N.; Allara, D. L. *J. Am. Chem. Soc.* **2002**, *124*, 5528. (b) Fisher, G. L.; Hooper, A. E.; Opila, R. L.; Allara, D. L.; Winograd, N. *J. Phys. Chem. B* **2000**, *104*, 3267.
(46) Long, N. *Metallocenes. An introduction to sandwich complexes*; Blackwell Science Ltd.: London, 1998.
(47) Gagne, R. R.; Koval, C. A.; Lisenky, G. C. *Inorg. Chem.* **1980**, *19*, 2855.
(48) Bashkin, J. K.; Kinlen, P. J. *Inorg. Chem.* **1990**, *29*, 4507.

purity, ESPI metals) onto clean glass substrates. Deposition base pressures were $\sim 5 \times 10^{-6}$ Torr and deposition rates were typically 0.1−1 nm/s. An oxide was formed by venting the chamber with ultrapure oxygen (Air Products) for 2−5 min and then venting to air. The substrates were immediately immersed for 3 h in 1−3 mM ethanolic solutions of 1,1′-ferrocenedicarboxylic acid (FDCA), ferrocenecarboxylic acid (FCA), 1, 4-dibenzoic acid (DBA), or 1,6-hexanedioic acid (HDA) (Sigma Aldrich). 1,9-Nonanedioic acid (NDA) monolayers were prepared by immersing substrates in 1−3 mM hexadecane solutions for 12−15 h. The substrates were then rinsed with solvent (absolute ethanol or chloroform) for 1−2 min and dried with high purity nitrogen. Self-assembly of molecules on 25 mm × 37 mm samples was confirmed using RAIRS.

An 80−100 nm aluminum electrode was deposited on top of the self-assembled molecules to allow electrical measurements. To minimize damage of the molecules, a slow deposition rate of ∼0.1 nm/10 s was used for the first 10 nm and a faster rate of 0.1−0.2 nm/s for the remaining ∼80 nm. Substrates were mounted on a water-cooled sample holder, thereby keeping sample temperatures below 70 °C during deposition of the top electrode. Depositions for PTJs intended for electrical characterizations were performed using ∼0.25 mm wide masks. Typical junction resistances were in the 1−50 kΩ range. Larger (25 mm × 37 mm) samples with semitransparent, 1.5−2.0 nm aluminum overlayers were prepared for RAIRS measurements.

A data acquisition card was used to apply tunnel junction bias voltages (V). Resulting currents (I) were converted to voltages using a commercial amplifier (Keithly 428 current amplifier), and the corresponding signal was recorded via the data acquisition card. Differential conductance readings at 0 V ($\sigma_{0V} = dI/dV|_{0V}$) were measured directly using a lock-in amplifier. $I-V$ measurements were performed at various temperatures using a homemade liquid nitrogen cryostat enclosed in a purged glovebag. Cyclic voltammetry of molecules in acetonitrile was performed in a standard one compartment cell under ambient atmosphere at 25 °C. Platinum wires were used as counter and working electrodes and a silver wire as a reference electrode. The electrochemical cell and a commercial current amplifier were interfaced with a data acquisition card, which was used as the voltammetric analyzer. Tetrabutylammonium hexafluorophosphate was the supporting electrolyte. All chemicals employed in this study were used as received from Sigma Aldrich, and solvents were ACS grade. RAIRS measurements were performed at an 80° incidence angle using a Nicolet Nexus 470 FTIR spectrometer equipped with a Spectra-Tech variable angle, specular reflectance accessory, a liquid nitrogen cooled MCT detector, and dry air purge.

Results

Cyclic voltammograms of a 1.5 mM FDCA acetonitrile solution, with an Fc/Fc^+ couple ($E° = 0.400$ V vs NHE) added as an internal standard, exhibited a reversible one-electron oxidation at $E_{1/2} = 0.46$ V (vs NHE) with a $\Delta E \sim 100$ mV.[48,49] The measurements were consistent over a series of 20 scans. Comparison with the reference Fc/Fc^+ couple indicated that oxidation of FDCA is made more difficult by the electron-withdrawing carboxylate substituents, as has been reported in the literature.[48,49]

Figure 1 shows RAIRS spectra of FCA and FDCA both before and after deposition of a ∼2 nm aluminum overlayer. RAIRS spectroscopy is an effective means to confirm self-assembly of FDCA molecules on aluminum/aluminum oxide surfaces and to probe potential chemical or structural changes that can occur after deposition of the aluminum overlayer. Representative spectra shown in Figure 1 were obtained using

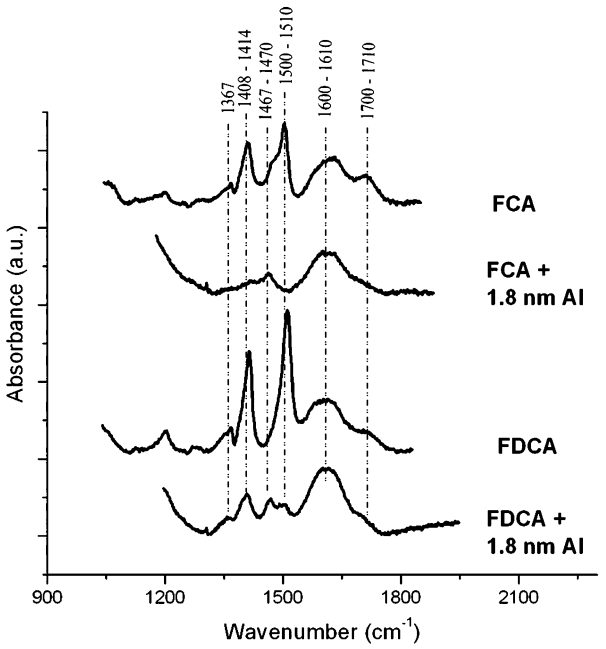

Figure 1. Reflection absorption infrared spectra (RAIRS) of FDCA and FCA on aluminum/aluminum oxide substrates before and after deposition of a 1.8 nm aluminum film.

freshly prepared samples. Spectra taken after several days showed an increase in intensity and considerable broadening of an aluminum oxide peak at 930 cm^{-1}, which tended to obscure signals due to the underlying molecules. The aluminum overlayer oxidizes upon exposure to air; however, the overlayer was sufficiently thin to permit spectroscopic investigations of the molecules underneath. NDA monolayers were also investigated in the same manner. Peak assignments for self-assembled monolayers are based on previous work performed using bulk FDCA,[50−52] ferrocene and benzoic acid derivatives on various surfaces,[53−59] and self-assembled alkanoic acids on aluminum oxide.[43−45, 60]

Before deposition of the aluminum overlayer, FDCA and FCA monolayers exhibit a broad shoulder at 1700−1730 cm^{-1} that is consistent with hydrogen-bonded and non-hydrogen-bonded carbonyl stretches.[60] Bands at 1600−1610 and 1467−1470 cm^{-1} are assigned to asymmetric and symmetric carboxylate stretching modes,[60] respectively, and the strong bands at 1500−1510 cm^{-1} are associated with an Fc ring/carbonyl combination mode.[52−54] Other Fc ring modes are observable at ∼1367 and 1408−1414 cm^{-1}. Aromatic and aliphatic C−H stretches at 3100 and 2930 cm^{-1}, respectively, were also observed for both FCA and FDCA monolayers.

Upon deposition of the aluminum overlayer, several changes in the RAIRS spectra indicate that, in all cases, the monolayers are significantly modified. The asymmetric carboxylate stretch

(49) Frosch, W.; Back, S.; Lang, H. *Organometallics* **1999**, *18*, 5725.
(50) Nomura, T. *Bull. Chem. Soc. Jpn.* **1983**, *56*, 2937.
(51) de Souza, A. C.; Pires, A. T. N.; Soldi, V. *J. Therm. Anal. Calorim.* **2002**, *70*, 405.
(52) Bodenheimer, J. S.; Low, W. *Spectrochim. Acta* **1973**, *29A*, 1733.
(53) Ye, S.; Sato, Y. Uosaki, K.; *Langmuir* **1997**, *13*, 3157.
(54) Popenoe, D. D.; Deinhammer, R. S.; Proter, M. D. *Langmuir* **1992**, *8*, 2521.
(55) (a) Sondag, A. H. M.; Raas, M. C.; Touwslager, F. J. *App. Surf. Sci.* **1991**, *47*, 205. (b) Sondag, A. H. M.; Raas, M. C. *J. Chem. Phys.* **1989**, *91*, 4926.
(56) Koutstaal, C. A.; Angevaare, P. A. J. M.; Ponec, V. *J. Catal.* **1993**, *143*, 573.
(57) Koutstaal, C. A.; Ponec, V. *Appl. Surf. Sci.* **1993**, *70/71*, 206.
(58) Han, S. W.; Seo, H.; Chung, Y. K.; Kim, K. *Langmuir* **2000**, *16*, 9493.
(59) Groff, R. P. *J. Catal.* **1983**, *79*, 259.
(60) Allara, D. L.; Nuzzo, R. G. *Langmuir* **1985**, *1*, 52.

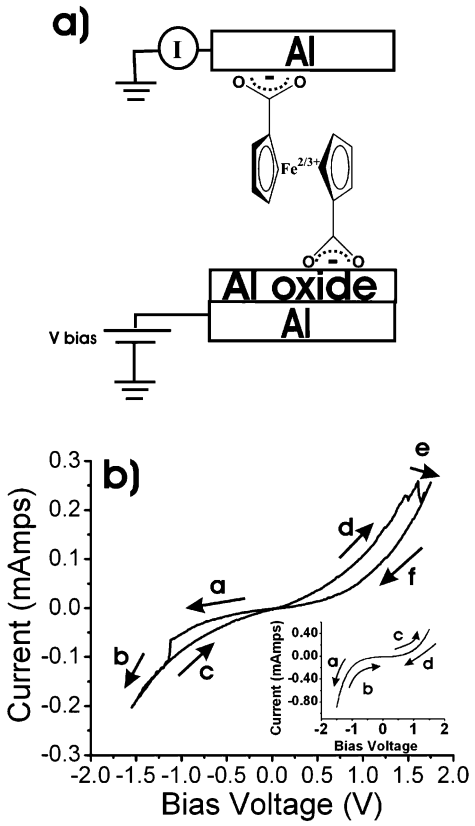

Figure 2. (a) An idealized schematic representation of tunnel junction experimental setup. (b) A typical $I-V$ curve at 210 K for an FDCA tunnel junction exhibiting reversible hysteretic behavior. (Inset) A typical $I-V$ curve at 210 K for an NDA tunnel junction. Arrows denote voltage sweep directions.

peaks become dominant features in spectra of FCA and FDCA films. Relative to the asymmetric carboxylate stretching mode intensity, carbonyl stretching mode intensities decrease by almost 50% for both FDCA and FCA monolayers and by about 80% for NDA monolayers. Features related to the Fc ring modes are almost entirely lost in the FCA spectra, and the spectra resemble those of buried NDA films. On the other hand, FDCA monolayers continue to exhibit most of the features attributed to the ring modes: features at ~1367, 1410, and 1500 cm^{-1} are still present, although they have decreased in intensity compared to the asymmetric carboxylate stretch. A band at ~1467 cm^{-1}, which can be attributed to the carboxylate symmetric stretching mode, becomes apparent in the FDCA spectrum after aluminum deposition.

An idealized schematic representation of the tunnel junction experimental setup is presented in Figure 2a. A bias voltage was applied to the initially deposited (bottom) aluminum electrode, and the top electrode was effectively grounded through the current amplifier. The bias voltage was scanned at a rate of 50−100 mV/s, and most measurements were obtained at 210 K, as discussed further below. A typical $I-V$ curve for a FDCA tunnel junction exhibiting stable and reversible hysteresis is shown in Figure 2b. The $I-V$ profile is divided into six regions (labeled a−f in Figure 2b). Starting from 0 V, the junction is scanned toward more negative voltages (region a). Before a threshold voltage is reached, the current varies in a smooth and nonlinear fashion with bias. Once the threshold voltage is reached, the current and differential conductance suddenly jump to higher values (region b) and eventually

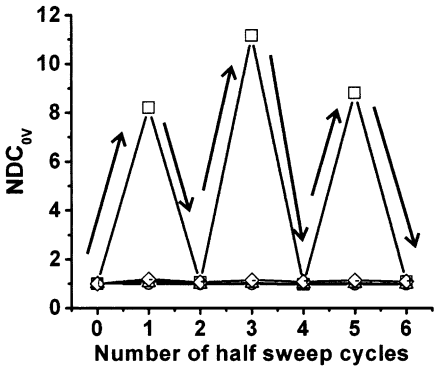

Figure 3. Normalized differential conductance at 0 V (NDC_{0V}) and 210 K obtained after several $\pm^1/_2$ half sweep cycles using as prepared junctions (△) and tunnel junctions doped with FDCA (□), FCA (▲), DBA(●), or NDA (○). Upward and downward arrows indicate negative and positive scan directions, respectively. Results for junctions other than those doped with FDCA are clustered around $NDC_{0V} \cong 1$. Data shown are averages over 15 junctions for FDCA and over least four junctions for each of the other systems.

stabilize as the voltage is made more negative. As the bias is swept back to 0 V (region c), the differential conductance remains at its higher value, and the current no longer traces its initial path. We refer to regions a−c as a $-^1/_2$ sweep cycle. Tunnel junctions that have undergone a $-^1/_2$ sweep cycle and that are subsequently subjected to negative bias voltages again trace the higher differential conductance path (region c). To restore such junctions to their original differential conductance state, the bias is swept toward positive voltages (region d). When a threshold voltage is reached, the current and differential conductance suddenly drop to lower values (region e). The differential conductance remains low as the voltage is increased further and is subsequently swept back toward 0 V (region f). We refer to regions d−f in Figure 2b as a $+^1/_2$ sweep cycle. If we begin with a $+^1/_2$ sweep cycle rather than a $-^1/_2$ sweep cycle, the junction remains in its low differential conductance state. We have tested over 30 junctions. While the behaviors of ~25% were similar to those of undoped junctions, more than 50% exhibit such strong hysteretic behavior and survived at least two $-^1/_2$ and two $+^1/_2$ sweep cycles. Some junctions exhibit as many as eight complete cycles. For control measurements, as prepared PTJs as well as junctions that contained FCA, HDA, NDA, or DBA were subjected to the same sweep cycles as the FDCA junctions. We tested at least four control junctions of each type and consistently observed $I-V$ curves as shown in the inset of Figure 2b. These junctions exhibited a much smaller hysteresis as discussed below. Similar small effects have been observed by others and have been attributed to trapped charges.[40,61]

Average zero bias normalized differential conductance ($NDC_{0V} = [dI/dV]/[dI/dV|_{0V}]$) for 15 different FDCA tunnel junctions over six $^1/_2$ sweep cycles are shown in Figure 3. NDC_{0V} was measured at 210 K using a lock-in amplifier before and after $-^1/_2$ and $+^1/_2$ sweep cycles. Each junction's initial differential conductance, that is before the junction was subjected to any $^1/_2$ sweep cycles, was used as the normalization factor when calculating respective NDC_{0V} values. After $-^1/_2$ sweep cycles, maximum NDC_{0V} values ranged from 2 to 20 and yielded an average maximum value of ~10. After a subsequent $+^1/_2$ sweep

(61) Handy, R. M. *Phys. Rev.* **1962**, *126*, 1968.

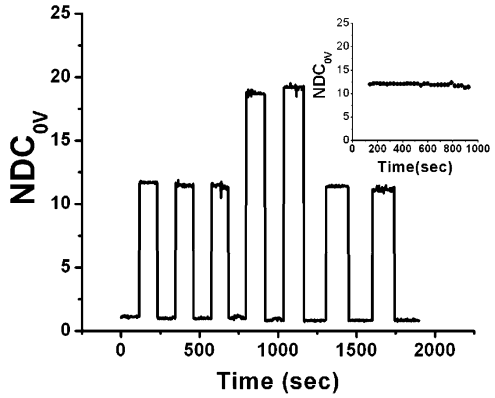

Figure 4. Normalized differential conductance at 0V (NDC_{0V}) vs time for high and low differential conductance states of FDCA tunnel junctions. (Inset) NDC_{0V} vs time for a high conductance state. Data were obtained at 210 K.

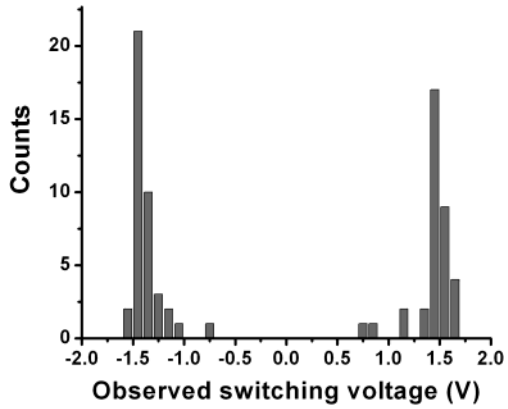

Figure 5. Histogram of conductance switching threshold voltages observed using FDCA tunnel junctions at 210 K.

cycle, the NDC_{0V} was restored to $\pm 5-10\%$ its original value. Results for junctions containing FCA, NDA, or DBA as well as those for as prepared junctions are also plotted in Figure 3. Points shown reflect average NDC_{0V} of at least four junctions of each type. At most, the NDC_{0V} values changed by $\sim 10\%$ after a $-1/2$ sweep cycle and were subsequently restored to about 1% of their original NDC_{0V} values by a subsequent $+1/2$ sweep cycle. That is, maximum NDC_{0V} changes of these control junctions were 2 orders of magnitude smaller than those typically exhibited by FDCA junctions.

Figure 4 shows NDC_{0V} behavior vs time over a period of ~ 2000 s. High and low differential conductance states were allowed to persist for 150 s before the junctions were subjected to an appropriate switching $\pm 1/2$ sweep cycle. Although high differential conductance NDC_{0V} values vary from cycle to cycle ($NDC_{0V} \sim 12$ and ~ 20), once switched, both high and low differential conductance states were stable over the 150 s time frame. The inset shows NDC_{0V} for a high differential conductance state over 1000 s. Over this time scale also, there is very little NDC_{0V} fluctuation provided that the temperature remains constant. We note that over substantially longer periods of time measurements using as prepared junctions show that oxide growth can lead to a significant drop in differential conductance.

A histogram of threshold switching voltages at 210 K is presented in Figure 5. Figure 5 was generated by tabulating the voltages at which sudden differential conductance changes occurred within a given $I-V$ curve for both $\pm 1/2$ sweep cycles. Figure 2b, for example, exhibits clear sudden changes at -1.1, $+1.5$, and $+1.6$ V. Low-to-high and high-to-low conductance switching voltages have average values of about -1.45 and 1.50 V, respectively. A distribution of threshold voltages likely arises from inhomogeneities in the native aluminum oxide. At lower temperatures higher threshold voltages were observed, whereas at higher temperatures junctions tended to show more frequent irreversible differential conductance increases after only one or two voltage sweep cycles. Thus to reduce difficulties due to localized heating and to obtain better yield and reproducibility, we performed most measurements at 210 K. Generally, the differential conductance of our tunnel junctions exhibited thermally assisted behavior, as has been observed by us and others in different systems.[11,32b] All junctions typically exhibited 0 V differential conductance drops of $\sim 30\%$ as the temperature was lowered from 298 to 211 K. The temperature dependence may arise from thermally assisted transport across metal−molecule interfacial barriers and nuclear motion.[11,32b]

Discussion

Cyclic voltammogram scans confirm a well-known reversibility of FDCA oxidation and reduction in solution. Numerous groups have already shown that Fc moieties can exhibit reversible oxidation and reduction once tethered to surfaces such as gold,[62−64] ITO,[65,66] and Si.[66b−d] In these systems, the electrolyte in solution makes a suitable electrical contact with the molecules on the surface such that they do not lose their electrochemical functionality.

To make an entirely solid state molecular electrical device, frequently a metal electrode is deposited on the molecules and care must be exercised to retain their functionality. RAIRS measurements performed before and after deposition of a thin, semitransparent metal overlayer provide an invaluable means to monitor chemical changes induced by the deposition. Before deposition of an aluminum overlayer, FDCA monolayer spectra exhibit a carbonyl stretching mode, implying free carboxylic acid groups. This is expected since, although some molecules may have both functional groups attached to the oxide surface, others will very likely have one carboxylic acid group free. The presence of the mode in FCA monolayer spectra suggests that some molecules may be physisorbed to the surface or may be hydrogen bonded with other molecules. A similar situation may occur in FDCA monolayers as well. However, the presence of the asymmetric carboxylate stretch peak in both FCA and FDCA monolayer spectra indicates that molecules can also chemisorb to the aluminum oxide surface. This is in agreement with infrared and inelastic tunneling studies of benzoic and alkanoic acids on aluminum oxide.[57,59,60] A symmetric carboxylate stretch mode is also observed and appears as a shoulder of the Fc ring/

(62) Chidsey, C. E. D.; Bertozzi, C. R.; Putvinski, T. M. Mujsce, A. M. *J. Am. Chem. Soc.* **1990**, *112*, 4301.
(63) Curtin, L. S.; Peck, S. R.; Tender, L. M.; Murray, R. W.; Rowe, G. K.; Creager, S. E. *Anal. Chem.* **1993**, *65*, 386.
(64) Berchmans, S.; Ramalechume, C.; Lakshmi, V.; Yegnaraman, V. *J. Mater. Chem.* **2002**, *12*, 2538.
(65) Zotti, G, Schiavon, G.; Zecchin, S.; Berlin, A.; Pagani, G. *Langmuir* **1998**, *14*, 1728.
(66) (a) Gardner, T. J.; Frisbie, C. D.; Wrighton, M. S. *J. Am. Chem. Soc.* **1995**, *117*, 6927. (b) Li, Q.; Mathur, G.; Homsi, M.; Surthi, S.; Misra, V.; Malinoskii, V.; Schweikart, K.-H.; Yu, L.; Lindsey, J.; Liu, Z.; Dabke, R. B.; Yasseri, A.; Bocian, D. F.; Kuhr, W. G. *Appl. Phys. Lett.* **2002**, *81*, 1494. (c) Liu, Z.; Yasseri, A. A.; Lindsey, J. S.; Bocian, D. F. *Science* **2003**, *302*, 1543. (d) Roth, K. M.; Yasseri, A. A.; Liu, Z.; Dabke, R. B.; Malinovskii, V.; Schweikart, K.-H.; Yu, L.; Tiznado, H.; Zaera, F.; Lindsey, J. S.; Kuhr, W. G.; Bocian, D. F. *J. Am. Chem. Soc.* **2003**, *125*, 505.

carbonyl combination peak in the FCA spectrum, further confirming chemisorption to the surface. The corresponding mode is difficult to discern in the FDCA spectrum. However, the Fc ring/carbonyl combination mode in the FDCA spectrum is very strong, likely due the free, second carboxylic acid group, and may be overshadowing symmetric carboxylate stretch. Strong peaks related to the in-plane Fc ring stretching modes[52] are observed in both the FCA and FDCA monolayer spectra, implying that molecules can have an appreciable perpendicular orientation.

After deposition of a ~2 nm aluminum film, spectra of both FCA and FDCA samples are significantly altered. In both cases, carbonyl stretching modes become weaker with respect to carboxylate asymmetric modes. For FCA monolayers, the aluminum may be percolating through the monolayer, reacting with previously unreacted carboxylic acid groups and potentially damaging molecules.[42−45] This picture is consistent with the observed dramatic attenuation of Fc ring modes and the dominance of carboxylate modes in the FCA monolayer spectrum. In principle, changes in Fc ring mode intensity can be induced by changes in molecular orientation with molecules surviving intact, but this is not likely the case here given the strength of the carboxylate mode, rigidity of the molecule, and the high reactivity of the deposited aluminum. A significant portion of the carbonyl mode attenuation in the FDCA spectra may be due to reaction of aluminum with free carboxylic acid groups of molecules chemisorbed to the surface via a carboxylate−aluminum oxide bond. This is consistent with the significant drop in the Fc ring/carbonyl combination peak relative to the carboxylate asymmetric peak. It is also consistent with the fact that FDCA monolayer continues to exhibit Fc ring modes even after the aluminum deposition. Thus, although it is likely that not all FDCA molecules are suitably oriented and survive the deposition intact, the second carboxylic acid group of the FDCA molecules seems to serve as a "protecting group" by reacting with incoming aluminum atoms and inhibiting their penetrating and damaging the underlying organic layer. Allara and co-workers have observed a similar effect using carboxylic acid terminated alkanethiols on gold.[43−45] The RAIRS results suggest that damage inflicted by the deposited aluminum to the FCA monolayer, and in particular to the Fc ring structure itself, can explain why FCA junctions did not exhibit strong differential conductance switching, even though FCA molecules are redox active in solution. Control measurements using as prepared junctions as well as junctions containing HDA, NDA, and DBA (that is, non-redox active molecules with two carboxylic acid groups) also did not reveal strong hysteretic switching.

Together, the results suggest that the differential conductance switching we observe using FDCA tunnel junctions likely arises from oxidation/reduction of protected ferrocene moieties that remain functional even after aluminum deposition. Initially, iron atoms in the FDCA junctions are expected to be in the Fe(II) state. During a $-^1/_2$ scan cycle, we reach a certain threshold voltage at which an electron is removed from the Fe(II), forming Fe(III), and the FDCA molecules are oxidized to form $FDCA^+$. The electron is transferred to the nearby top, more positive electrode, and a sudden differential conductance increase is observed. The molecules retain their oxidized state as the bias voltage is returned to zero, and the junction remains in its high differential conductance state. Sweeping the voltage to positive

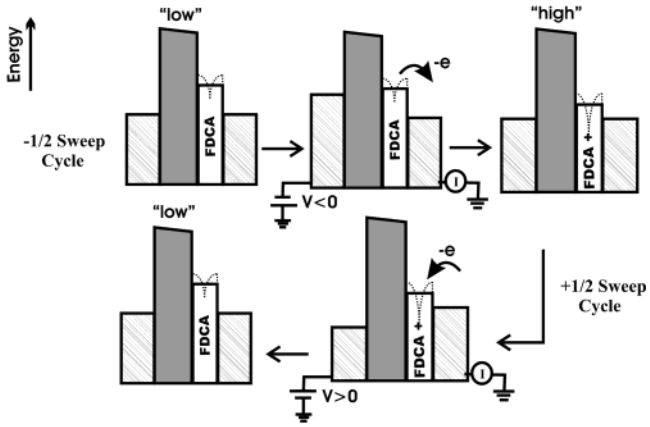

Figure 6. Effective average barrier model for FDCA/$FDCA^+$ tunnel junctions. Dashed lines sketch a potential due to charge distribution in ferrocene moiety. Hatched and shaded areas denote aluminum electrodes and aluminum oxide, respectively.

values during the $+^1/_2$ scan cycle reduces $FDCA^+$ back to FDCA beyond a threshold voltage. The differential conductance then suddenly drops, and the junction remains in its low conductance state as the bias is returned to zero volts.

In view of the structure of molecules used in control measurements, which did not exhibit strong reversible hysteretic changes in differential conductance, and since large changes in differential conductance in FDCA junctions are observed even at *zero bias*, we can use an effective barrier model presented in Figure 6 to rationalize the large switching observed. In Figure 6, the oxide is represented by a large trapezoidal barrier. Unoccupied molecular orbitals of FDCA are approximated as a continuous conduction band and are represented by a smaller barrier. Additional barriers may also be present at the interfaces and have been purported to contribute temperature-dependent behavior in other systems.[32b] Charge transfer occurs at the metal−oxide interface to equilibrate chemical potentials[2] and at the molecule−oxide and molecule−metal interfaces to form bonds.[43−45] The presence of such charged species (e.g., COO^-) implies that the various barriers are not necessarily flat as shown schematically in Figure 6 and that $I-V$ curves can be asymmetric with respect to the sign of the bias (for example, see NDA control junction data shown in Figure 2b, inset). In electrochemical cells, changes in barrier profiles due to potential induced motion of such charged species has been observed using long, flexible redox active molecules tethered to electrodes.[67] However, our control measurements using HDA, NDA, and DBA suggest that this effect cannot account for the large differential conductance changes observed for FDCA tunnel junctions. The molecules considered here are likely either not flexible enough or their motion is strongly constrained in the tunnel junction due to interactions with electrodes and/or other molecules.

Our results suggest that when a sufficiently negative bias is applied to the bottom electrode, electrons in the FDCA molecules are repelled, $FDCA^+$ is formed, and charge is transferred to the nearby, relatively more positive top electrode. The resulting *positive* charges in the molecules create a new electric field which is expected to lower the effective molecular barrier for electron tunneling when the bias is returned to 0 V. In bulk

(67) Wang, X.; Kharitonov, A. B.; Katz, E.; Willner, I. *Chem. Commun.* **2003**, *13*, 1542.

systems, the modified field also gives rise to an observed lowering of the first excited state energy of ferrocenium with respect to that of ferrocene (2.0 vs 2.7 eV, respectively).[68−70] A lower molecular barrier increases the overall transmission and differential conductance of a tunnel junction since transmission in a WKB approximation is given by the product of the transmissions through the oxide and the molecules separately.[11] Note that a positive charge on the molecules is expected to make hole transport more difficult and lower differential conductance if holes were the dominant charge carriers. Cycling the bottom electrode to sufficiently positive potentials reduces the $FDCA^+$ back to FDCA through injection of electrons from the top electrode, lowering differential conductance again. In contrast, current flowing through non-redox active regions of the film should contribute a background that varies smoothly with voltage.

The above-mentioned reversibility and stability of Fc oxidation and reduction states may prove advantageous for molecular based memory applications. The system also provides a valuable test bed for clarifying detailed mechanisms relating to charge-transfer models. Typically, such models involve a number of complex factors such as electronic coupling between the charge donor and acceptor, density of states of the metal, free energy for charge exchange, and reorganization energies, including those related to nuclear rearrangement.[71] Charge transfer involving solutions have been extensively studied, and the importance of a number of additional factors has been elucidated.[37,63,72,73] Solvent effects contribute significantly to the reorganization energy. Also, charge flow is strongly influenced by ion dynamics, which are in turn influenced by interactions of ions with other ions and with the environment.[72] In the present experiment, the solvent has been replaced with a solid state, metal electrode, which leads to some simplifications as well as further complications. For instance, on one hand, current flow through metals can be straightforwardly described and reorganization energies may be modeled using image charge methods.[74] On the other hand, a close proximity of metal electrodes leads to a number of important questions, such as the nature of the coupling between the molecule and electrodes,[32b,75,76] their effect on molecular states,[77] the degree of charge displacement or polarization effects induced at the interfaces as the junction is formed,[16−19] and the nature molecular configurations at buried interfaces.[43−45] Such questions relating the nature of metal−molecule contacts naturally arise in a full development of molecular electronics and are particularly important for nanometer scale systems. Well-defined oxidation−reduction states of organometallic compounds combined with the sensitivity of PTJ systems should provide a useful new platform for exploring these issues.

Conclusions

We have shown that FDCA molecules can mediate ∼10-fold, stable, reversible differential conductance switching in aluminum oxide/aluminum planar tunnel junctions. Control measurements performed with molecules that do not include two carboxylic groups or do not include a ferrocene moiety also do not exhibit the switching. Infrared measurements suggest that the carboxylic groups in FDCA serve to bind molecules to the oxide and to protect them from the overlaid aluminum electrode. Combined, the results indicate that observed switching likely arises from the oxidation and reduction of protected ferrocene moieties.

Acknowledgment. This work was supported by the Natural Science and Engineering Council for Canada, the Canadian Foundation for Innovation, and the Ontario Innovation Trust.

Supporting Information Available: Detailed tunnel junction experimental setup and representative $I-V$ scans of FDCA and control junctions. This material is available free of charge via the Internet at http://pubs.acs.org.

JA0394176

(68) Sohn, Y. S.; Hendrickson, D. N.; Gray, H. B. *J. Am. Chem. Soc.* **1970**, *92*, 3233.
(69) Sohn, Y. S.; Hendrickson, D. N.; Smith, J. H.; Gray, H. B. *Chem. Phys. Lett.* **1970**, *6*, 499.
(70) Sohn, Y. S.; Hendrickson, D. N.; Gray, H. B. *J. Am. Chem. Soc.* **1971**, *93*, 3603.
(71) (a) Marcus, R. A. *J. Chem. Phys.* **1965**, *43*, 679. (b) Marcus, A. A. *J. Phys. Chem*. **1990**, *94*, 1050.
(72) Sumner, J. J.; Creager, S. E. *J. Phys. Chem. B* **2001**, *105*, 8739.
(73) Chidsey, C. E. D. *Science* **1991**, *251*, 919.
(74) Simmons, J. G. *J. Appl. Phys.* **1963**, *34*, 1793.
(75) Nitzan, A. *Annu. Rev. Phys. Chem.* **2001**, *52*, 681.
(76) Kaun, C.-C.; Larade, B.; Guo, H. *Phys. Rev. B* **2003**, *67*, 121411-1.
(77) Tian, W.; Datta, S.; Hong, S.; Reifenberger, R.; Henderson, J. I.; Kubiak, C. P. *J. Chem. Phys.* **1998**, *109*, 2874.